EMISSION MECHANISMS IN A PHOTOCATHODE RF GUN*

J. H. Han†, J. Bähr, H.-J. Grabosch, M. Krasilnikov, V. Miltchev, A. Oppelt, B. Petrosyan,
S. Riemann, L. Staykov, F. Stephan, DESY, D-15738 Zeuthen, Germany
M. V. Hartrott, BESSY GmbH, D-12489 Berlin, Germany
K. Flöttmann, S. Schreiber, DESY, D-22607 Hamburg, Germany
J. Rönsch, Hamburg University, D-22761 Hamburg, Germany
P. Michelato, L. Monaco, D. Sertore, INFN Milano-LASA, I-20090 Segrate (MI), Italy

Abstract

In photocathode rf guns, emission mechanisms at the photocathode play a crucial role in the overall beam dynamics. An electron beam with a low bunch charge as well as a short laser pulse length allow to study the emission mechanisms with a good phase definition and with a very small influence of the space charge force. This paper presents experimental and numerical studies toward detailed understanding of the photo emission and secondary emission processes at the Cs_2Te cathode.

INTRODUCTION

High gain FELs demand very high quality electron beams with an emittance below 1 mm mrad at 1 nC [1]. This emittance is close to the value limited by the thermal emittance [2]. In order to decrease the limit defined by the emission mechanisms of photocathodes, a detailed understanding of the processes at the cathode are essential. Characterizing parameters of photoemission are quantum efficiency (QE), kinetic energy of the photoelectrons, and response time between the impact of the drive laser photon and the extraction of the photoelectrons. Secondary emission can be parameterized in terms of secondary yield and response time between primary and secondary electrons.

Cs_2Te has a band gap E_{G} of 3.3 eV and an electron affinity E_{A} of 0.2 eV when produced under ultrahigh vacuum conditions [3]. Even though the emission parameters are partly known [4], these parameters are not constant during gun operation but modified by the rf field strength as well as contaminations of the surface. Therefore, the emission mechanisms under gun operation conditions must be found.

In this article, the bunch charge and the thermal emittance in dependence on the accelerating field in the PITZ gun cavity [5] under operation conditions are discussed for a Cs_2Te cathode (#43.2 [6]). In extension of Ref. [7] the secondary emission depending on the gun gradient is studied for the same cathode. The cathode consists of a Mo cathode plug of 8 mm radius, which is partially covered with a Cs_2Te film (2.5 mm radius and 30 nm thickness). The cathode was quite new (not used for normal operation) and showed relatively low dark current [8].

* This work has been partly supported by the European Community contract RII3-CT-2004-506008 and by the 'Impuls- und Vernetzungsfonds' of the Helmholtz Association contract VH-FZ-005.

† jang.hui.han@desy.de

BEAM DYNAMICS

Figure 1 shows the extracted beam charge as a function of the emission phase. For these measurements, a short (3 ps rms) Gaussian laser pulse has been used to produce a small amount of charge (max. 9 pC). The measurements have been made with a Faraday cup 78 cm downstream of the cathode and the data have been read with an oscilloscope in the control room. Due to the small signal-to-noise ratio for low charge measurements, the error is of the order of several percent. The numbers on the plots denote the maximum rf field at the cathode. Beam charge measurements were made with a scan of the emission phase.

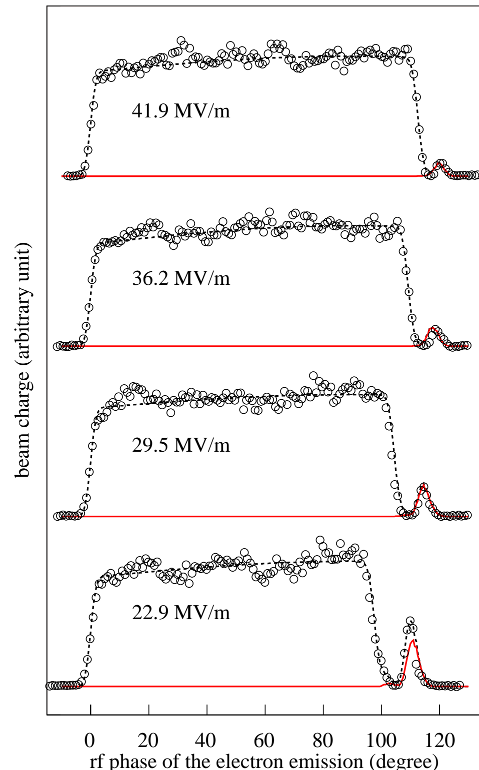

Figure 1: Beam charge vs. the rf phase of the electron emission for different rf input power levels (see text).

The steep increase of the bunch charge around 0° is related to the pulse shape of the drive laser [9], while the slow increase of the charge between ∼10° and ∼90° is due to the Schottky effect. After ∼90°, the electrons cannot be

efficiently accelerated by the rf field due to strong phase slippage [7]. The corresponding simulations (dotted black line) include the photo-emitted electrons as well as the secondary electrons. The secondary electrons (solid red line) are also shown separately.

PHOTOEMISSION

Schottky effect

With increasing field strength at the surface of the cathode, a barrier defined by the electron affinity is lowered. This is called the Schottky effect. The variation of the electron affinity under operation conditions may change the photo-emission as well as field emission properties. Spicer's relation [10] based on the three-step model can be applied to explain the field dependence of the photo-emitted bunch charge:

$$Q_{\rm bunch} = \frac{G\,[h\nu - (E_{\rm A} + E_{\rm G})]^{\frac{3}{2}}}{[h\nu - (E_{\rm A} + E_{\rm G})]^{\frac{3}{2}} + \Gamma}, \qquad (1)$$

where G and Γ are fit parameters to be determined from experimental data. The photon energy $h\nu$ of the drive laser is 4.75 eV in this study.

When a new Cs_2Te cathode is inserted into the gun, the QE decreases down to $\sim$1% within some hours or days, where it then stays for month. This behavior can be explained by an increase of the electron affinity to $\kappa E_{\rm A,0}$, where $E_{\rm A,0}$ is the electron affinity of a uncontaminated cathode and κ is a parameter introduced to describe the contamination. The contamination parameter κ is close to 1 when the cathode is new and becomes larger with contamination.

On the other hand, the electron affinity is lowered by the rf field due to the Schottky effect by an amount of $\sqrt{\frac{e^3}{4\pi\epsilon_0}\beta_{\rm ph}E_{\rm emit}}$ [11], where $E_{\rm emit}$ is the rf field strength at the emission phase, and $\beta_{\rm ph}$ is the field enhancement factor for photoemission. $\beta_{\rm ph}$ includes geometrical effects and the polarization of the Cs_2Te film. Therefore, the $E_{\rm A}$ in Eq. 1 is re-written as

$$E_{\rm A} = \kappa E_{\rm A,0} - \sqrt{\frac{e^3}{4\pi\epsilon_0}\,\beta_{\rm ph}\,E_{\rm emit}}\,. \qquad (2)$$

For the emission phase between 10° and 80° at the four different rf strength cases in Fig. 1, the beam charges were collected and plotted in Fig. 2 to find the fit parameters, κ, $\beta_{\rm ph}$, G, and Γ. The fit has been made using Eq. 1 and 2: $\kappa = 2.2$, $\beta_{\rm ph} = 3$, $G = 11.7$, and $\Gamma = 0.59$. From the fit result in Fig. 2, the bunch charge increase at the 0 – 4 MV/m range is $\sim$8% with 262 nm photon wavelength. Coleman [12] reported $\sim$13% increase at the same field strength range with 254 nm photon wavelength. This discrepancy is possibly due to Cs_2Te thickness. For a thiner layer, a smaller Schottky effect is expected. The large measurement error and the absence of data points at low rf field strength can contribute to the discrepancy as well.

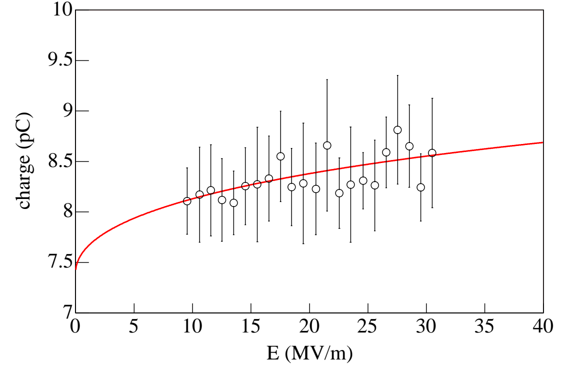

Figure 2: Beam charge vs. the rf field strength at the emission phase. The beam charges have been collected by scanning the emission phase at several rf input power levels.

Thermal emittance

The kinetic energy of the photoelectrons defines the thermal emittance as [13]

$$\varepsilon^{\rm therm}_{n,\rm rms} = r_{\rm rms}\sqrt{\frac{2\,E_{\rm kin}}{m_0c^2}}\,\frac{1}{\sqrt{3}} \times\sqrt{\frac{2+\cos^3\phi_{\rm max} - 3\cos\phi_{\rm max}}{2\,(1-\cos\phi_{\rm max})}}, \qquad (3)$$

where

$$\cos\phi_{\rm max} = \sqrt{\frac{E_{\rm A}}{E_{\rm kin}}} \qquad (4)$$

and $r_{\rm rms}$ is the rms transverse size of the emitted bunch which is estimated from a measurement of the laser spot size. The measurement procedure is described in Ref. [2].

Even though the measurement has been performed with a small charge (3 pC) electron beam generated by a short laser pulse (3 ps rms Gaussian), the measured emittance (black circle in Fig. 3) includes several contributions.

$$\varepsilon_{\rm meas} = \sqrt{\left(\varepsilon^{\rm therm}_{\rm real}\right)^2 + \left(\varepsilon^{\rm rf}\right)^2 + \left(\varepsilon^{\rm sys.error}_{\rm slit.meas}\right)^2}. \qquad (5)$$

In addition, we have to introduce a constant η to describe a discrepancy between our measurements and the theoretical model as:

$$\varepsilon^{\rm therm}_{\rm real} = \eta\,\varepsilon^{\rm therm}_{\rm theo}. \qquad (6)$$

η may be related to measurement errors due to laser jitter (position and intensity) or of the laser spot size or rf jitter (power and phase), or may be a real emittance contribution due to a non-uniform QE or mechanical roughness of the photo cathode. In this study, η has been set to 1.47 for the fit shown in Fig. 3. Future studies will concentrate on a better understanding and possibly a reduction of the parameter η.

The rf emittance $\varepsilon^{\rm rf}$, has its origin in the transverse and longitudinal size of the bunch. In Fig. 3, $\varepsilon^{\rm rf}$ has been numerically calculated with ASTRA [14] with the machine parameters for each measurement points.

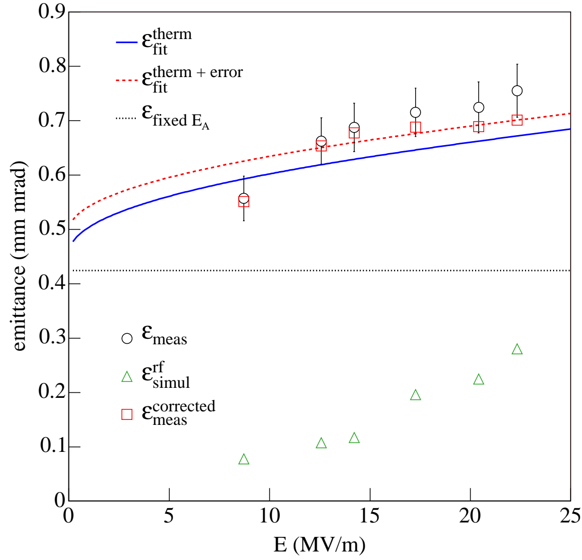

Figure 3: Transverse emittance at 0.55 mm rms size of the laser pulse and 3 pC bunch charge vs. the rf field strength at the emission phase (see text). In order to find a corrected emittance $\varepsilon_{\rm meas}^{\rm corrected}$ (□) the simulated rf emittance $\varepsilon^{\rm rf}$ (△) has been subtracted from the measured emittance $\varepsilon_{\rm meas}$ (◯). This corrected emittance includes the real thermal emittance $\varepsilon_{\rm real}^{\rm therm}$ and the systematic error of the slit measurement $\varepsilon_{\rm slit.meas}^{\rm sys.error}$. An analytic estimate $\varepsilon_{\rm fit}^{\rm therm}$ with (- -) and without (–) systematic error $\varepsilon_{\rm slit.meas}^{\rm sys.error}$ has been made using Eq. 3 and 6. An analytic value using Eq. 3 with fixed $E_{\rm A}$ of 0.2 eV is shown for comparison.

$\varepsilon_{\rm slit.meas}^{\rm sys.error}$ is the systematic error in the slit measurement. This term is hard to separate from η. In this study, it has been set to 0.2 mm mrad according to an analysis of the position jitter of the beamlets and Fig. 5 in Ref [2] with a further consideration of the rf emittance.

SECONDARY EMISSION

If a primary electron strikes a solid material, it may generate secondary electrons. The secondary electron emission process is summarized in an empirical formula [15] which relates the energy of the primary electrons to the number of secondary electrons escaping from the surface:

$$\delta(E_p) = \delta_{\max} \frac{E_p}{E_{p,\max}} \frac{s}{s - 1 + (E_p/E_{p,\max})^s}, \qquad (7)$$

where $\delta(E_p)$ is the secondary emission yield depending on the energy of the primary, $\delta_{\max}$ is the maximum secondary yield, which occurs at the primary electron energy $E_{p,\max}$, and s is a fit parameter larger than 1, which describes the form of the secondary emission yield curve. In this study, the secondary emission parameters were taken from Ref. [7]: $\delta_{\max}$ = 7.0, $E_{p,\max}$ = 2.2 keV, and s = 1.5. A more detaied discussion can be found in Ref [7].

At an impact energy lower than $E_{p,\max}$, the electron penetration depth decreases with decreasing E_p and secondary electrons are generated within the range of the escape depth. At impact energies above $E_{p,\max}$, the penetration depth exceeds the escape depth so that some of the generated secondary electrons cannot reach the surface and the secondary yield decreases with increasing E_p. This behavior is found in Fig. 1. At the lowest gradient case (22.9 MV/m) the bump composed of the photoemission and the secondary emission electrons is relatively high, which means the impact energy of the primary electrons is close to $E_{p,\max}$. As the gradient increases, the impact energy exceeds $E_{p,\max}$ and the secondary electron yield shrinks.

DISCUSSION

At the maximum rf field of 42 MV/m (operating condition of PITZ1 and TTF2), the real thermal emittance $\varepsilon_{\rm real}^{\rm therm}$ is expected ∼0.7 mm mrad at 0.55 mm rms laser spot size. When neglecting that the electron affinity becomes negative, the $\varepsilon_{\rm real}^{\rm therm}$ is estimated as ∼0.6 mm mrad at 0.45 mm rms spot size for the XFEL (60 MV/m max field). Future studies will concentrate on a better understanding and possibly a reduction of the parameter η, which describes the discrepancy between measurement and model. In order to reduce the thermal emittance further an increase of the electron affinity by changing the Cs–Te ratio or additional surface layers on the cathode can be considered.

For a low charge beam, the effect of secondary electrons becomes weaker with increasing gradient. But, further studies are necessary for the case of high charge emission. Because the space charge force during the emission is comparable to the rf field, electrons can move backward to the cathode and produce secondary electrons.

REFERENCES

[1] The beam parameters of the European XFEL are described at http://xfel.desy.de/.

[2] V. Miltchev *et al.*, Proc. FEL 2004, p. 399.

[3] R. A. Powell *et al.*, Phys. Rev. B **8**, 3987 (1973).

[4] D. Sertore *et al.*, Proc. EPAC 2004, p. 408.

[5] M. Krasilnikov *et al.*, the present proceedings, WPAP006.

[6] Information on the photocathode is available at http://wwwlasa.mi.infn.it/ttfcathodes/.

[7] J. H. Han, M. Krasilnikov, and K. Flöttmann, Phys. Rev. ST Accel. Beams **8**, 033501 (2005).

[8] J. H. Han *et al.*, the present proceedings, WPAP004.

[9] S. Schreiber *et al.*, Proc. FEL 1999, p. **II**-69.

[10] W. E. Spicer, Phys. Rev. **112**, 114 (1958).

[11] R. Gomer, *Field emission and field ionization*, (American Institute of Physics, 1993).

[12] C. I. Coleman, Appl. Optics **17**, 1789 (1978).

[13] K. Flöttmann, TESLA-FEL 97-01 (1997).

[14] K. Flöttmann, A Space Charge Tracking Algorithm (ASTRA), http://www.desy.de/∼mpyflo/.

[15] M. A. Furman and M. T. F. Pivi, Phys. Rev. ST Accel. Beams **5**, 124404 (2002).